ZOOLOGICAL RESEARCH

Hydroxycoumarin efficiently inhibits spring viraemia of carp virus infection *in vitro* and *in vivo*

Lei Liu[1,2,3], Da-Wei Song[1,2,3], Guang-Lu Liu[4], Li-Peng Shan[1,2,3], Tian-Xiu Qiu[1,2,3], Jiong Chen[1,2,3,*]

[1] *State Key Laboratory for Managing Biotic and Chemical Threats to the Quality and Safety of Agro-products*, *Ningbo University*, *Ningbo*, *Zhejiang* 315211, *China*

[2] *Laboratory of Biochemistry and Molecular Biology*, *School of Marine Sciences*, *Meishan Campus*, *Ningbo University*, *Ningbo*, *Zhejiang* 315832, *China*

[3] *Key Laboratory of Applied Marine Biotechnology of Ministry of Education*, *Meishan Campus*, *Ningbo University*, *Ningbo*, *Zhejiang* 315832, *China*

[4] *School of Chemistry* & *Chemical Engineering*, *Zhoukou Normal University*, *Zhoukou*, *Henan* 466001, *China*

ABSTRACT

Spring viremia of carp virus (SVCV) causes devastating losses in aquaculture. Coumarin has an advantageous structure for the design of novel antiviral agents with high affinity and specificity. In this study, we evaluated a hydroxycoumarin medicine, i.e., 7-(6-benzimidazole) coumarin (C10), regarding its anti-SVCV effects *in vitro* and *in vivo*. Results showed that up to 12.5 mg/L C10 significantly inhibited SVCV replication in the epithelioma papulosum cyprini (EPC) cell line, with a maximum inhibitory rate of >97%. Furthermore, C10 significantly reduced cell death and relieved cellular morphological damage in SVCV-infected cells. Decreased mitochondrial membrane potential (ΔΨm) also suggested that C10 not only protected mitochondria, but also reduced apoptosis in SVCV-infected cells. For *in vivo* studies, intraperitoneal injection of C10 resulted in an anti-SVCV effect and substantially enhanced the survival rate of virus-infected zebrafish. Furthermore, C10 significantly enhanced antioxidant enzyme activities and decreased reactive oxygen species (ROS) to maintain antioxidant-oxidant balance within the host, thereby contributing to inhibition of SVCV replication. The up-regulation of six interferon (IFN)-related genes also demonstrated that C10 indirectly activated IFNs for the clearance of SVCV in zebrafish. This was beneficial for the continuous maintenance of antiviral effects because of the low viral loads in fish. Thus, C10 is suggested as a therapeutic agent with great potential against SVCV infection in aquaculture.

Keywords: Antiviral effect; Spring viraemia of carp virus; Interferon response; Antioxidant-oxidant balance

INTRODUCTION

Artificial pressures on aquatic ecosystems can lead to the

Received: 10 February 2020; Accepted: 24 April 2020; Online: 10 May 2020

Foundation items: This work was supported by the Program for the National Natural Science Foundation of China (31902410), Natural Science Foundation of Ningbo City of China (2019A610419), General Scientific Research Project of Education of Zhejiang Province (Y201839187), Scientific Innovation Team Project of Ningbo (2015C110018), Scientific Research Fund of Ningbo University (XYL19017), and K.C. Wong Magna Fund in Ningbo University

*Corresponding author, E-mail: jchen1975@163.com

DOI: 10.24272/j.issn.2095-8137.2020.037

emergence and outbreak of different diseases in fish. The aquacultural industry is vulnerable to significant economic losses associated with disease, such as viral infections for which there are no efficacious treatments or preventative measures (Balmer et al., 2018; Fujioka et al., 2015). Spring viremia of carp (SVC) is an acute and contagious hemorrhagic disease in cyprinids caused by the spring viremia of carp virus (SVCV), which is a notifiable pathogen on the list of the World Organization for Animal Health (formerly Office International des Epizooties, OIE) (Ahne et al., 2002). SVCV belongs to the family Rhabdoviridae and infects most cyprinids, including common carp (*Cyprinus carpio*), goldfish (*Carassius auratus*), grass carp (*Ctenopharyngodon idella*), bighead carp (*Aristichthys nobilis*), rainbow trout (*Oncorhynchus mykiss*), and fathead minnow (*Pimephales promelas*) (Ashraf et al., 2016; Petty et al., 2002). With global trade transporting large quantities of live fish between countries, SVCV has spread to Europe (Fijan, 1984), North America (Dikkeboom et al., 2004; Garver et al., 2007), and Asia (Chen et al., 2006; Teng et al., 2007), and poses a serious threat to the carp industry; for example, 4 000 metric tons of carp are lost in Europe each year (Miller et al., 2007). Therefore, the development of antiviral agents that can be applied for prophylactic or therapeutic treatment against SVCV in aquaculture remains a crucial issue.

Coumarin (benzo-α-pyrone) is an oxygen heterocycle and the parent chemical structure for a class of phytochemicals naturally occurring in several plants. Coumarin is also regarded as an advantageous structure for the design of novel antiviral agents with high affinity and specificity to various molecular targets (Penta, 2015). Research on coumarin derivatives has developed rapidly following isolation from natural material as well as classical and combinatorial synthesis (Hassan et al., 2016). Based on the correlation between structural characteristics and biological activities, synthetic coumarins with a variety of pharmacophoric groups at the C-3, C-4, and C-7 positions have been screened intensively for antiviral effects. Numerous coumarins have been evaluated for inhibition against human immunodeficiency virus (HIV) replication, such as 4-hydroxycoumarin analogue warfarin (Bourinbaiar et al., 1993; Stubbs & Bode, 1993), tricyclic pyranocoumarins suksdofin and pteryxin (Huang et al., 1994a, 1994b), and furanocoumarin imperatorin (Sancho et al., 2004). In addition, several promising coumarins, including imidazopyridine-coumarin, purine-coumarin, and benzoxazole-coumarin, have shown substantial anti-hepatitis virus activity at half maximal effective concentrations (EC_{50}) of 6.8, 2.0, and 12 μmol/L, respectively (Neyts et al., 2009).

In aquaculture, some hybrid coumarin derivatives have been synthesized to reduce SVCV loads *in vitro* and *in vivo*, exhibiting potential application against SVCV infection (Liu et al., 2019a, 2019b, 2020). Previous study has shown that coumarin groups with linker lengths of three, four, and six carbon atoms have a higher inhibitory effect on SVCV (Liu et al., 2017). These findings provide a series of coumarins with potential anti-SVCV properties. In the present study, we investigated 7-(6-benzimidazole) coumarin (C10) and identified antiviral effects on SVCV infection *in vitro* through apoptosis assay and observations of nucleus damage and cell ultrastructure. C10 showed a similar structural composition as the groups mentioned above, with six carbon atoms in the linker or imidazole groups, and therefore demonstrated a similar structural activity relationship with SVCV. Our findings indicated that C10 had a remarkable effect on the formation and scavenging of reactive oxygen species (ROS), and thus, influenced processes involving free radical-mediated injury. Follow-up *in vivo* study suggested that C10 could be suitable as a possible therapeutic agent for SVCV in aquaculture.

MATERIALS AND METHODS

Cell, virus, and fish

Epithelioma papulosum cyprini (EPC) cells were cultured in medium 199 (M199) (Hyclone, USA), supplemented with 10% fetal bovine serum (FBS) (Every Green, China), penicillin (100 IU/mL), and streptomycin (0.1 mg/mL) (Beyotime, China) and maintained at 25 °C.

The SVCV strain (0504) was isolated from common carp (Chen et al., 2006) and kindly provided by Prof. Qiang Li (Key Laboratory of Mariculture, Agriculture Ministry, PRC, Dalian Ocean University, Dalian, China). The strain was then propagated in EPC cells containing M199 supplemented with 2% FBS until a cytopathic effect (CPE) was observed. Subsequently, the virus was harvested and stored at –80 °C until further use. The virus was titrated into 96-well plates and 50% tissue culture infective dose ($TCID_{50}$) analysis was performed according to the Reed-Muench method (Pizzi, 1950).

Due to their easy susceptibility to SVCV infection (Encinas et al., 2013), adult zebrafish (*Danio rerio*) are considered an ideal experimental model for studying the antiviral effect of medicines on SVCV *in vivo* (Liu et al., 2019; Shen et al., 2018; Shen et al., 2019; Qiu et al., 2020). Zebrafish (total length 3.17±0.24 cm, body weight 0.61±0.23 g, mean±*SD*) were purchased from the Beilun Aquatic Breeding Center (Ningbo, China), maintained in a static water system consisting of four 200 L aquarium ponds at 20 °C, and fed commercial fresh blood worms thrice per day. Ten zebrafish were randomly selected to verify SVCV-free status, as described previously (Koutná et al., 2003). Prior to *in vivo* tests, experimental fish were transferred into new containers and acclimatized at 15 °C for one week. All experiments are performed according to the Experimental Animal Management Law of China and approved by the Animal Ethics Committee of Ningbo University.

Synthesis of hydroxycoumarin C10

The detailed synthesis route of C10 is shown in Figure 1. Briefly, 7-hydroxycoumarin (8.1 g, 50 mmol) in acetone (150.0 mL) was added to anhydrous K_2CO_3 (13.8 g, 100.0 mmol) and KI (200.0 mg) with stirring for 30 min at room temperature. Afterwards, 1,6-dibromotexane (14.6 g, 60.0 mmol) was mixed

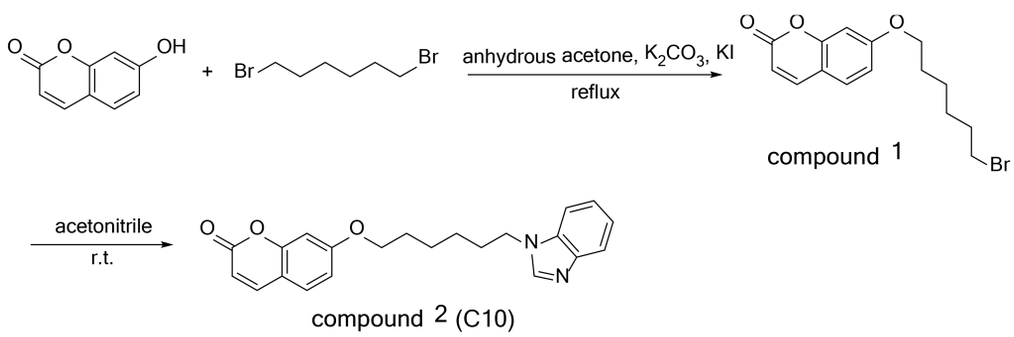

Figure 1 Synthetic route of C10 (r.t. is room temperature)

into the reaction and refluxed at 60 °C for 24 h. The precipitate was then filtered and washed with acetone (400.0 mL), and the organic layer was combined and concentrated. Purification was performed via silica gel column chromatography with mixed petroleum ether and ethyl acetate (5:1, v/v) as the eluent, resulting in compound 1,7-(6-bromohexyloxy) coumarin (8.9 g) (yield 54.6%). To synthesize compound 2, a mixture containing 7-(6-bromohexyloxy) coumarin (650.6 mg, 2.0 mmol) with benzimidazole (472.6 mg, 4.0 mmol) and anhydrous K_2CO_3 (1.4 g, 10.0 mmol) was stirred at room temperature for 24 h. After filtering and evaporation, the organic layer was dried and concentrated. The residue was purified using silica gel chromatography with chloroform/methanol (10:1) as the eluent to obtain compound 2 (i.e., C10) as a white solid (529.3 mg) with a yield of 73.1%. C10 was dissolved in dimethyl sulfoxide (DMSO) and used at the indicated concentrations.

Cell cytotoxicity and *in vitro* inhibition assays of C10

Cell viability assays were performed with a Cell Counting Kit-8 (CCK-8, Beyotime, China), which used WST-8, a water-soluble tetrazolium dye, to enhance sensitivity of the WST-8-based assay over conventional 3-(4,5-dimethylthiazol-2-yl)-5-(3-carboxymethoxyphenyl)-2-(4-sulfophenyl)-2H-tetrazolium (MTS)-based assay. Briefly, serial dilutions of C10 in M199 supplemented with 2% FBS, at concentrations of 0.4 mg/L to 25.0 mg/L (in triplicate), were added to EPC cells in 96-well plates. After every 24 h, cell viability assays using CCK-8 were performed as per the manufacturer's protocols. After 2 h of incubation at 37 °C, colorimetric absorbance from the mitochondrial enzyme substrate reaction was measured at 450 nm using a microplate reader (ELX800, Gene, Hong Kong, China). As DMSO exhibits no cytotoxicity at doses up to 0.1% (v/v) (Liu et al., 2020), signals were compared to solvent-treated cells (DMSO up to 0.05%, v/v).

Antiviral activity assays were performed as per previous research (Liu et al., 2017). Briefly, EPC cells seeded on 12-well and 96-well plates were infected with SVCV at 10^3×$TCID_{50}$/mL at 25 °C, followed by the addition of serial dilutions of C10. After 48 h of infection, the antiviral activity of C10 against SVCV replication in EPC cells was tested by quantitative real-time polymerase chain reaction (qRT-PCR) and CCK-8.

Cell morphology evaluation and ultrastructural analysis

The sampled cells were harvested and maintained in 2.5% glutaraldehyde at 4 °C overnight. The sampled cells were prepared for scanning (SEM) and transmission electron microscopy (TEM) as described in previous studies (Liu et al., 2015; Zhang et al., 2011). Cells were observed using SEM (Hitachi, Japan) and ultrathin sections were observed using TEM (1200EX TEM, JEOL, Japan).

Time-of-addition and time-of-removal assays

EPC cells in 12-well plates were incubated with SVCV for 1 h at 25 °C to allow the virus to both attach to and enter cells. The virus was removed, and cells were washed twice with M199 medium before the addition of fresh media. At various viral replication time points (i.e., 0, 2, 4, 6, 8, 12, 18, and 24 h post-infection (hpi)), up to 12.5 mg/L C10 was introduced to assess its effects on SVCV infection under time-of-addition study. For time-of-removal, SVCV-infected cells were exposed to 12.5 mg/L C10 at 0 hpi. At the same time points as above, the medium containing C10 was replaced with cell culture maintenance medium. Infected cell cultures were treated with 0.025% DMSO as the control and all samples were harvested at 24 hpi, and the related expression of SVCV protein N was analyzed by RT-qPCR. Triplicate wells were used for each treatment at each time point.

Effects of C10 on SVCV-induced apoptosis

EPC cells were incubated with SVCV (10^3×$TCID_{50}$/mL) and 12.5 mg/L C10 at 25 °C for 48 h. After incubation, the cells were washed thrice with phosphate-buffered saline (PBS) and treated with 2-(4-amidinophenyl)-6-indolecarbamidine dihydrochloride (DAPI) (1 mg/L) and 1,1'-dioctadecyl-3,3,3',3'-tetramethylindocarbocyanine perchlorate (Dil) (5 mg/mL). Fluorescence signals were monitored using upright fluorescence microscopy (NI-U; Nikon, Japan). Additionally, apoptosis of the sampled cells was enumerated using a mitochondrial membrane potential assay kit with 5,5',6,6'-tetrachloro-1, 1',3,3'-tetraethylbenzimidazole-carbocyanide iodine (JC-1) (Beyotime, China) according to the manufacturer's instructions. As an ideal fluorescent probe, JC-1 generates a matrix of mitochondrion-forming aggregates that produce a red color when ΔΨm levels are high, whereas lower ΔΨm transforms JC-1 to its monomeric form, resulting in a green color. Fluorescence intensity was measured using a

MACSQuant 10 Analyzer, and a minimum of 10 000 cells were counted in each treatment.

Effects of C10 on ROS generation

We used 2',7'-dichlorodihydrofluorescein diacetate (DCFH-DA) and dihydroethidium (DHE) oxidant-sensitive probes to assess intracellular ROS levels. Briefly, EPC cells seeded on 12-well plates with coverslips were infected with SVCV in the presence of C10 at a concentration of 12.5 mg/L. The samples of SVCV-infected and C10-treated cells were harvested and incubated with 10 μmol/L DCFH-DA and 5 μmol/L DHE following the instructions provided in the kits (Beyotime, China). Fluorescence signals were monitored using an upright fluorescence microscope (NI-U; Nikon, Japan).

***In vivo* inhibition**

Zebrafish were randomly selected and separated into four aquaria containing UV-sterilized water. The rearing temperature of each aquarium was maintained at 15 °C. The experimental fish were intraperitoneally injected with 20 μL 10^4×$TCID_{50}$/mL SVCV. After 12 h, SVCV-infected fish were injected intraperitoneally with 50 mg/L C10 to test survival over an additional 7 d, and thus calculate mortality. The DMSO vehicle control was set at 0.1% (final concentration). To avoid deterioration of water quality, dead fish were immediately removed from the water.

Under the same operational procedures, three virus-infected and C10-treated fish were collected at 24 h, 48 h, and 96 h, and frozen at –80 °C until RNA and protein extraction. Exposure was conducted in static water with aeration. The fish were humanely euthanized with 40 μg/mL (final concentration) tricaine methanesulfonate (MS-222). The sampled fish were thawed and homogenized with 10 volumes of M199 using a stomacher or manual homogenization under ice-bath cooling. The homogenates were subjected to low-speed centrifugation at 2 000 g for 10 min at 4 °C. The virion in the supernatants was filtered through 0.45 μm membranes (Millipore, USA). The viral loads were detected using $TCID_{50}$ analysis.

Oxidative stress assays

The harvested cell and tissue samples were immediately extracted with cold PBS (0.1 mol/L, pH 7.4) in a cool ice-bath. The homogenates were centrifuged at 10 000 *g* for 15 min at 4 °C to obtain supernatants. Total protein content of the supernatants was determined using the Bradford method (Bradford, 1976) with bovine serum albumin (Beyotime Institute of Biotechnology, China). Four common antioxidant indices, i.e., glutathione (GSH), superoxide dismutase (SOD), total antioxidant capacity (T-AOC), and malondialdehyde (MDA), were measured using commercial assay kits (Jiancheng Institute and Beyotime, China) according to the manufacturer's instructions. All measurements were recorded on a microplate reader.

Total RNA extraction and viral load quantification

The samples were collected and immediately frozen in liquid nitrogen for subsequent RNA isolation. Total RNA was extracted using TRIZOL reagent (Takara, Japan) following the manufacturer's protocols, and subsequently eluted in 10–40 μL nuclease-free water for storage at –80 °C. Nucleic acid concentrations were quantified using a NanoDrop spectrophotometer (ThermoFisher, USA). Extracted RNA purity was determined using the A_{260nm}/A_{280nm} ratio with absorbance at 260 and 280 nm between 1.8 and 2.0, respectively. A total of 500 ng/μL of purified RNA was used for cDNA generation per reaction, which was reverse transcribed using HiScript Q Select RT SuperMix for qPCR (Vazyme, China). RT-qPCR was performed using ChamQ™ SYBR® qPCR Green Master Mix (Vazyme, China) in an ABI StepOnePlus™ Real-Time PCR Detection System (ThermoFisher, USA). PCR analysis was amplified as follows: 95 °C for 30 s, denaturation with 40 cycles at 95 °C for 15 s, and annealing at 60 °C for 60 s. To assess the specificity of each amplicon, melt curve analysis was also performed at the end of each thermal profile. The primer sequences are listed in Table 1. Each individual sample was run in triplicate.

Statistical analysis

Relative mRNA expression levels were calculated using the $2^{-\triangle\triangle Ct}$ method with the formula $\triangle\triangle Ct=(C_{t,\ target\ gene}-C_{t,\ reference\ gene})-(C_{t,\ target\ gene}-C_{t,\ reference\ gene})_{control}$ (Livak & Schmittgen, 2001). Drug response curves were represented by a logistic sigmoidal function with a maximal effect level (Amax) and Hill coefficient representing the sigmoidal transition (Origin 8.1, USA). Virus titers were log10 transformed prior to statistical analyses. For the experiments, unpaired Student's *t*-tests were used to compare significant differences between drug-treated and negative-control DMSO samples (SPSS 18.0, USA), presented as mean±*SD*. A Kaplan-Meier test was used for the survival rate of zebrafish. *P*-values of less than 0.05 were considered statistically significant.

RESULTS

Identification of C10

The ^{1}H NMR spectrum, ^{13}C NMR spectrum, and ESI-MS mass-to-charge ratio (*m*/*z*) were used to identify the structure of C10. The data are as follows: ^{1}H NMR (500 MHz, MeOD-d4) δ 8.16 (s, 1H), 7.75–7.73 (d, 1H, J=9.5 Hz), 7.69–7.67 (d, 1H, J=7.5 Hz), 7.62–7.60 (dd, 1H, J=6.0, 3.1 Hz), 7.51–7.49 (d, 1H, J=7.8 Hz), 7.40–7.38 (d, 1H, J=8.6 Hz), 7.31–7.24 (m, 1H), 6.79–6.77 (dd, 1H, J=8.5, 2.1 Hz), 6.73–6.72 (d, 1H, J=1.7 Hz), 6.18–6.16 (d, 1H, J=9.5 Hz), 4.23–4.20 (t, 2H), 3.91–3.88 (t, 2H), 1.86–1.83 (m, 2H), 1.70–1.67 (m, 2H), 1.45–1.42 (m, 2H), 1.32–1.24 (m, 2H); ^{13}C NMR (126 MHz, MeOD-d4) δ 163.83, 163.25, 156.97, 145.61, 144.59, 142.44, 130.28, 124.18, 123.74, 123.44, 120.12, 116.15, 114.05, 113.14, 111.42, 102.01, 69.43, 45.82, 30.70, 29.78, 27.35, 26.53; ESI-MS *m*/*z*, 363.52 $[M+H]^+$.

Cytotoxicity of C10 in EPC cells

The potential cytotoxicity of C10 was quantitatively assessed using the CCK-8 test. EPC cells were exposed to increasing concentrations of C10. No cytotoxicity was evident with

Table 1 Sequences of primer pairs used for analysis of gene expression by RT-qPCR

Gene		Primer sequence (from 5' to 3')
EPC-actin	Forward	GCTATGTGGCTCTTGACTTCGA
	Reverse	CCGTCAGGCAGCTCATAGCT
SVCV glycoprotein (G)	Forward	GCTACATCGCATTCCTTTTGC
	Reverse	GCTGAATTACAGGTTGCCATGAT
SVCV nucleoprotein (N)	Forward	AACAGCGCGTCTTACATGC
	Reverse	CTAAGGCGTAAGCCATCAGC
SVCV phosphoprotein (P)	Forward	TGAGGAGGAATGGGAATCAG
	Reverse	AGCTGACTGTCGGGAGATGT
SVCV matrix protein (M)	Forward	ATTCGGTCAAATGCCTCCTT
	Reverse	GCCTATCTTTTCCCCGTTTA
Fish-18S	Forward	ACCACCCACAGAATCGAGAAA
	Reverse	GCCTGCGGCTTAATTTGACT
ISG15	Forward	ACTCGGTGGTGATGCTCCTC
	Reverse	CCTTCGGCACTCTCTCTTTC
IFNγ	Forward	ATGATTGCGCAACACATGAT
	Reverse	ATCTTTCAGGATTCGCAGGA
RIG-I	Forward	TTGAGGAGCTGCATGAACAC
	Reverse	CCGCTTGAATCTCCTCAGAC
MHC-II	Forward	ATCTGCTAAAACTTTTTCTTGCC
	Reverse	GAACCCTACACACTTCACCTCTG
aoc2	Forward	GCATAAAGATGAAGAGCAGACCA
	Reverse	ATGTGTAGGAAACCAGCAGTGAC
Mx	Forward	ATAGGAGACCAAAGCTCGGGAAAG
	Reverse	ATTCTCCCATGCCACCTATCTTGG

exposure up to 12.5 mg/L C10 for 4 d (Figure 2), whereas cytotoxicity was observed at an exposure of 25 mg/L C10 at all time points.

Anti-SVCV effects of C10 *in vitro*

In this study, six-point dose antiviral responses of C10 *in vitro* were determined by RT-qPCR on the expression of four viral proteins (N/P/G/M). C10 was effective at inhibiting SVCV infection *in vitro* in a dose-dependent manner (Figure 3A). Results showed a maximum antiviral response of >97% in the 12.5 mg/L group. There was also significant inhibition of infection in supernatants with 1.6, 3.2, and 6.3 mg/L C10 and complete inhibition at 12.5 mg/L C10 (SVCV titer not detected) (Figure 3B), indicating that new viral particle formation was reduced. Inhibition of infection was increased when SVCV-infected cells were incubated with 6.3 and 12.5 mg/L C10 (Figure 3C, D), exhibiting a non-significant CPE in viral-infected cells. Additionally, incomplete cytomembranes and nuclear fragmentation were shown in SVCV-infected cells, which were weakened with 12.5 mg/L C10 treatment along with the disappearance of apoptotic bodies (Figure 3E).

The scanning electron micrographs in Figure 4A show that normal cells in the control were intact, round, and plump, and maintained a spherical shape and intact cytomembrane. After 48 h of SVCV infection, serious damage occurred in the cells, including cell shrinkage, volume reduction, and breakdown of cellular surface structure. However, due to the significant inhibition of infection, C10-treated cells were similar to that of the control, with normal growth characteristics, extrinsic morphology, and clear edges. Consistent with the results above, electron micrographs of intrinsic ultrastructure showed the majority of cells with typical characteristics of apoptosis, such as lower electron density area, aggravation of irregular borders, cytoplasmic vacuoles, and decreased mitochondria in

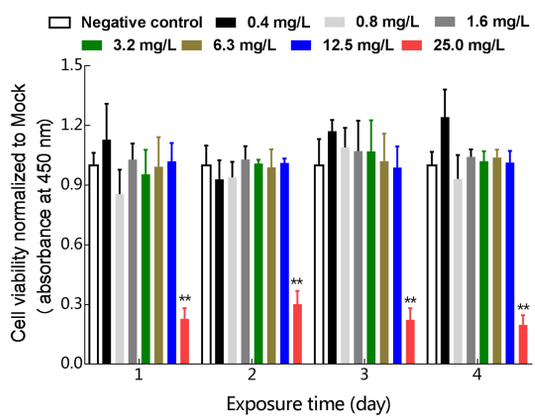

Figure 2 Cytotoxicity of C10 in EPC cells

C10 exhibited no cytotoxicity up to 12.5 mg/L over 4 d exposure. Each value is represented as mean±*SD* normalized to values for no treatment. *P*-values for each study were determined by Student's *t*-tests. **: $P<0.01$; *: $P<0.05$.

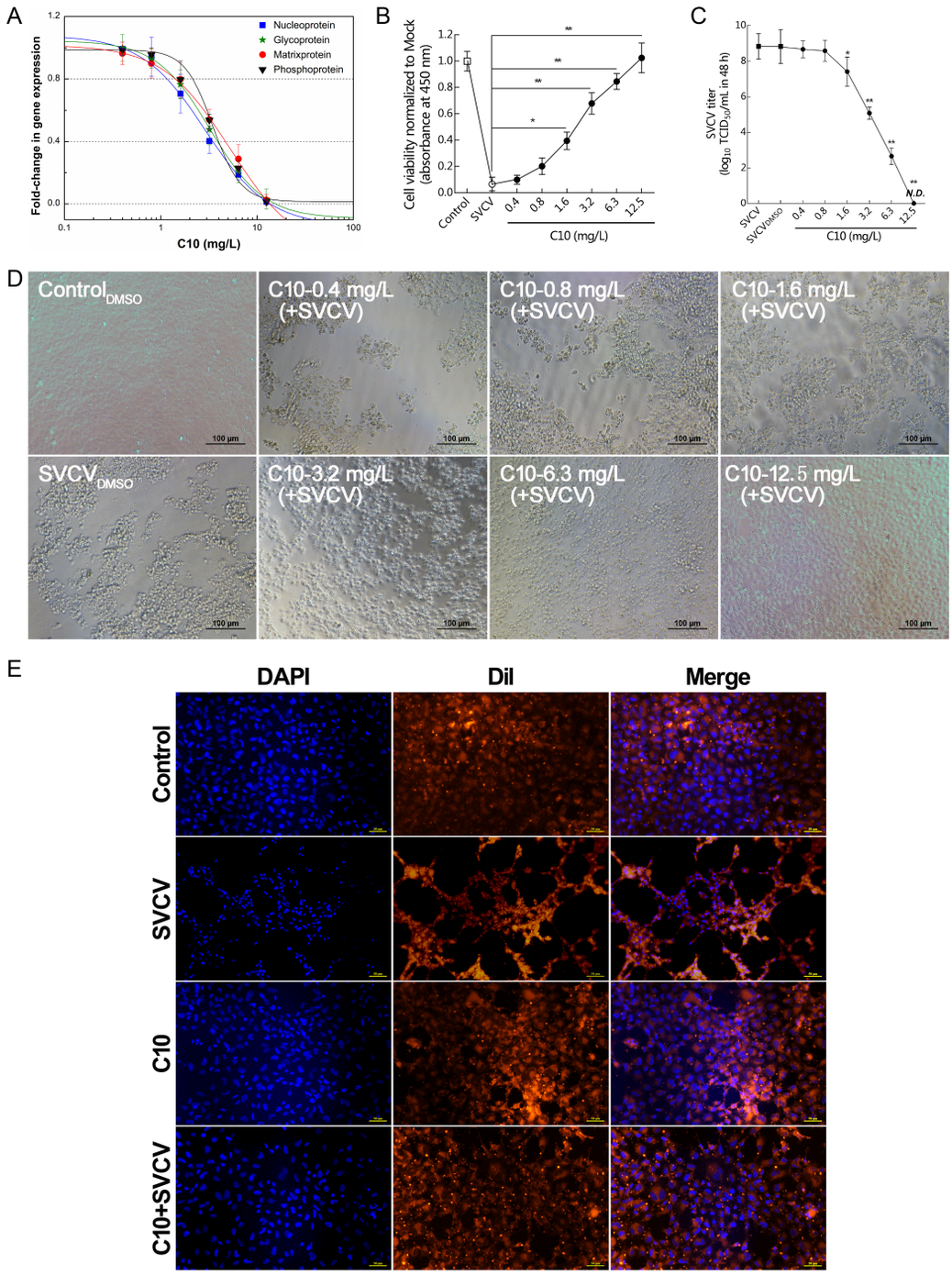

Figure 3 Antiviral effects of C10 *in vitro*

A: Six-point dose-response curves for antiviral activity of C10 in EPC cells. Percentages of inhibition on nucleoprotein, glycoprotein, matrix protein, and phosphoprotein expression were analyzed by RT-qPCR. Each sample was run in triplicate and normalized to β-actin. β-actin gene was used as an internal control for normalization, with relative expression represented as fold induction relative to expression level in positive control (SVCV without C10 treatment) (set to 1). B: Viral titers in supernatants of SVCV-infected and C10-treated cells. Viral titers were determined by $TCID_{50}$ analysis at 48 h based on Reed-Muench method. C and D: Morphological effects and cell viability of C10 were tested on SVCV infection in EPC cells. E: Apoptotic bodies were induced by SVCV infection. Each value is mean±*SD* normalized to values for no treatment. *P*-values for each study were determined by Student's *t*-tests. **: $P<0.01$; *: $P<0.05$.

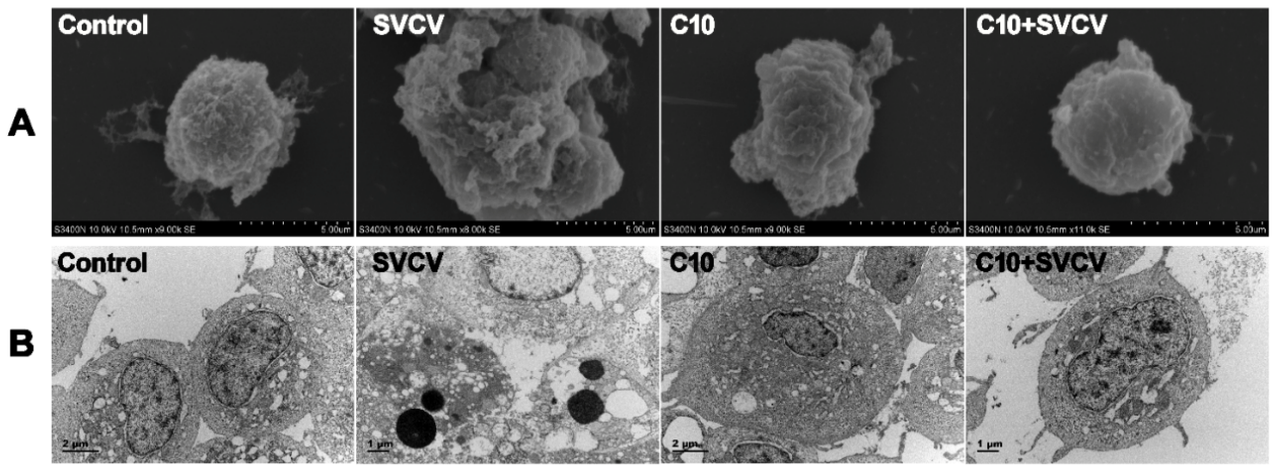

Figure 4 Cell morphology and ultrastructural analyses of C10 in SVCV-infected cells

A: Scanning electron microscopy image showing morphological effects of SVCV infection and antiviral activity of 12.5 mg/L C10 at 48 h. B: Ultrastructural changes in EPC cells and SVCV particles treated with 12.5 mg/L C10 at 48 h.

cytoplasm with SVCV infection (Figure 4B). Additionally, SVCV infection reduced the number of mitochondria and caused mitochondrial disruption, suggesting that SVCV destroys mitochondria to induce apoptosis in EPC cells. In contrast, there was no significant difference between the control and C10-treated cells. Together, these findings demonstrated that C10 at a concentration of 12.5 mg/L inhibited SVCV replication in target cells.

To characterize the role of C10 treatment on the SVCV replication cycle, time-of-addition and time-of-removal tests were performed with C10 on target cells. As shown in Figure 5, delays in C10 addition resulted in a gradual enhancement of protein N expression. Two sharp increases of

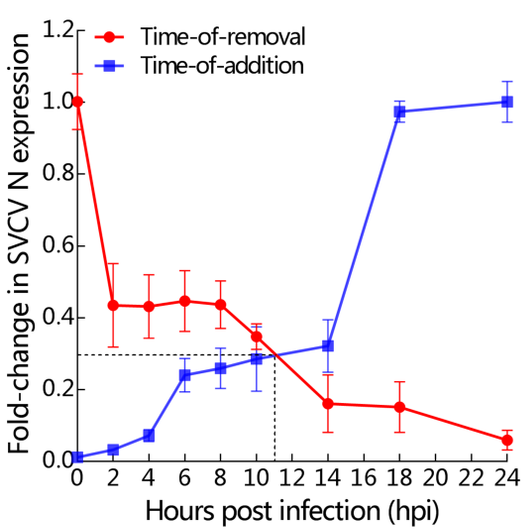

Figure 5 Effects of C10 on SVCV replication cycle

Relative RNA levels of N gene were determined by RT-qPCR from time-of-addition and time-of-removal tests. Interception point occurs between 10 and 12 hpi.

16.8% and 65.2% were observed from 4 hpi to 6 hpi and from 14 hpi to 18 hpi, respectively. Correspondingly, protein N expression gradually decreased with removal of C10 exposure, and a significant reduction occurred between 0 hpi and 2 hpi. According to the interception point of the time-of-addition and time-of-removal curves at 10–12 hpi, we concluded that the effect of C10 against SVCV replication was on viral biosynthesis.

Effects of C10 on mitochondrial membrane potential (ΔΨm)

A long-lasting drop or rise in normal ΔΨm levels may induce unwanted loss of cell viability and various pathologies (Zorova et al., 2018). A decrease in mitochondrial membrane potential is a sign of early stage apoptosis (Wang et al., 2008). In the present study, we evaluated whether C10 possesses antiviral activity against SVCV at normal ΔΨm levels. As shown in Figure 6, transformation between red and green was induced by SVCV at 24 h and remained stable until 48 h, whereas the levels in the C10 treatments showed no obvious change compared with levels in the control. Taken together, these data indicate that virus-induced apoptosis may be suppressed by C10.

Antioxidant-oxidant balance assays *in vitro* and *in vivo*

As hydroxycoumarin medicines generally possess antioxidant activity involving free radical-mediated injury (Peng et al., 2013), we hypothesized that C10 may protect the host against SVCV by recovering antioxidant activities in EPC cells and zebrafish. Strong fluorescence of DCFH-DA and DHE was present in the EPC cells of the viral group, whereas ROS generation following C10 treatment decreased significantly (Figure 7). Consistent with this hypothesis, the data in Figure 8A–C show that three antioxidant indices, i.e., GSH, SOD, and T-AOC, increased significantly in the C10 group versus the SVCV-infected group at 24 h and 48 h. Although independent C10 treatment did not increase the antioxidant

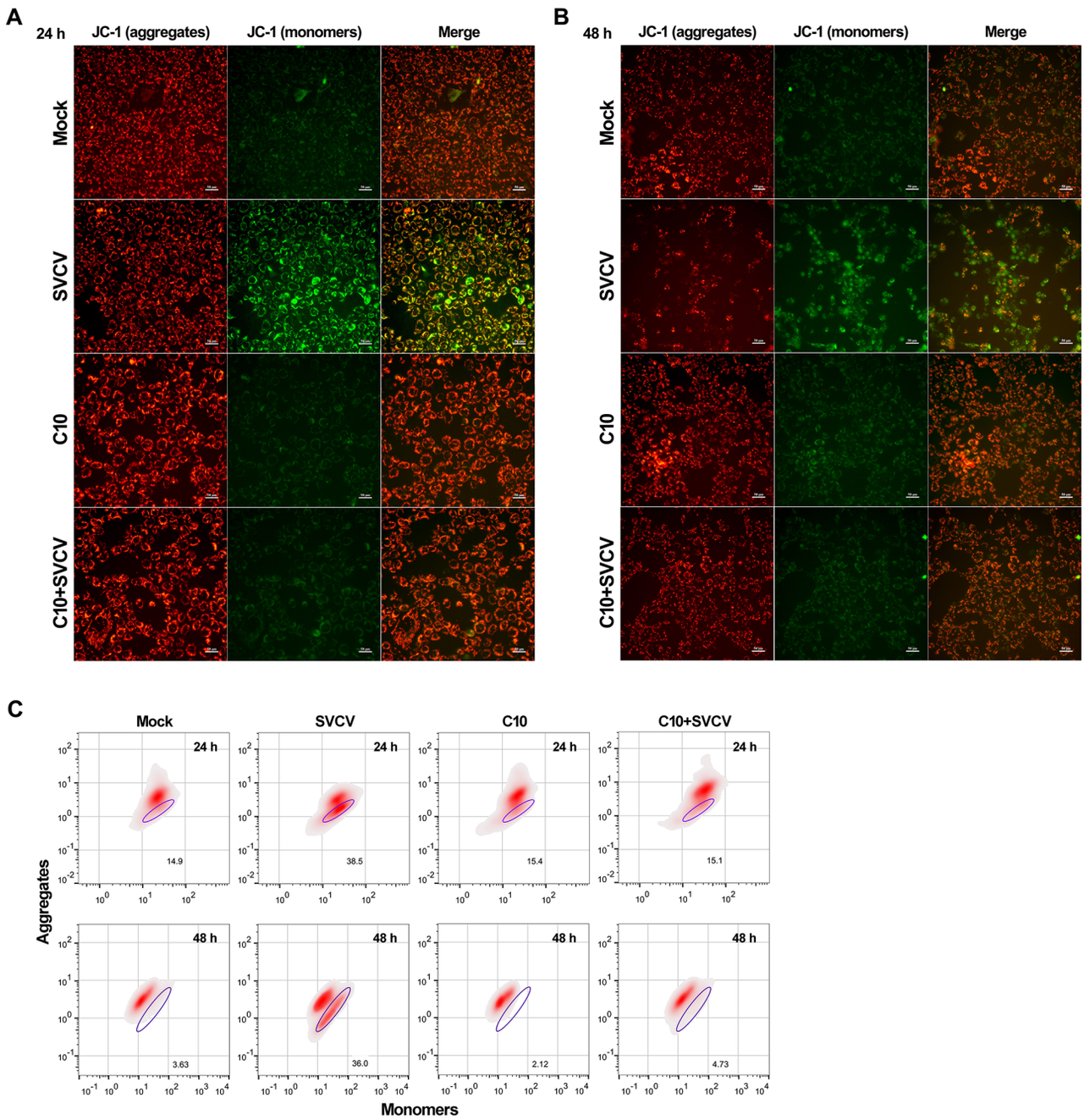

Figure 6 Effects of C10 on mitochondrial membrane potential (ΔΨm)

A, B: ΔΨm levels are shown. EPC cells in 12-well plates were treated in presence or absence of 12.5 mg/L C10 with SVCV infection at 24 h and 48 h. JC-1 is an ideal fluorescent probe, when ΔΨm levels are high, matrix of mitochondrion-forming aggregates turns red; whereas when ΔΨm levels are low, JC-1 is transformed to its monomeric form and turns green. C: Ratio of SVCV-induced apoptotic cells was detected using JC-1 staining at 24 h and 48 h.

capacities of the cells, it nevertheless reduced SVCV-induced MDA content by more than 40% at 24 h and 48 h (Figure 8D). Somewhat similar to the *in vitro* results, C10 also markedly promoted the responses of antioxidant activities in SVCV-infected zebrafish and exhibited oxidant resistance to SVCV infection (Figure 9).

Anti-SVCV effects of C10 *in vivo*

For *in vivo* study, clinical signs were used to assess the potential toxicity of C10. Based on preliminary toxicity experiments (data not shown), no signs of toxicity were

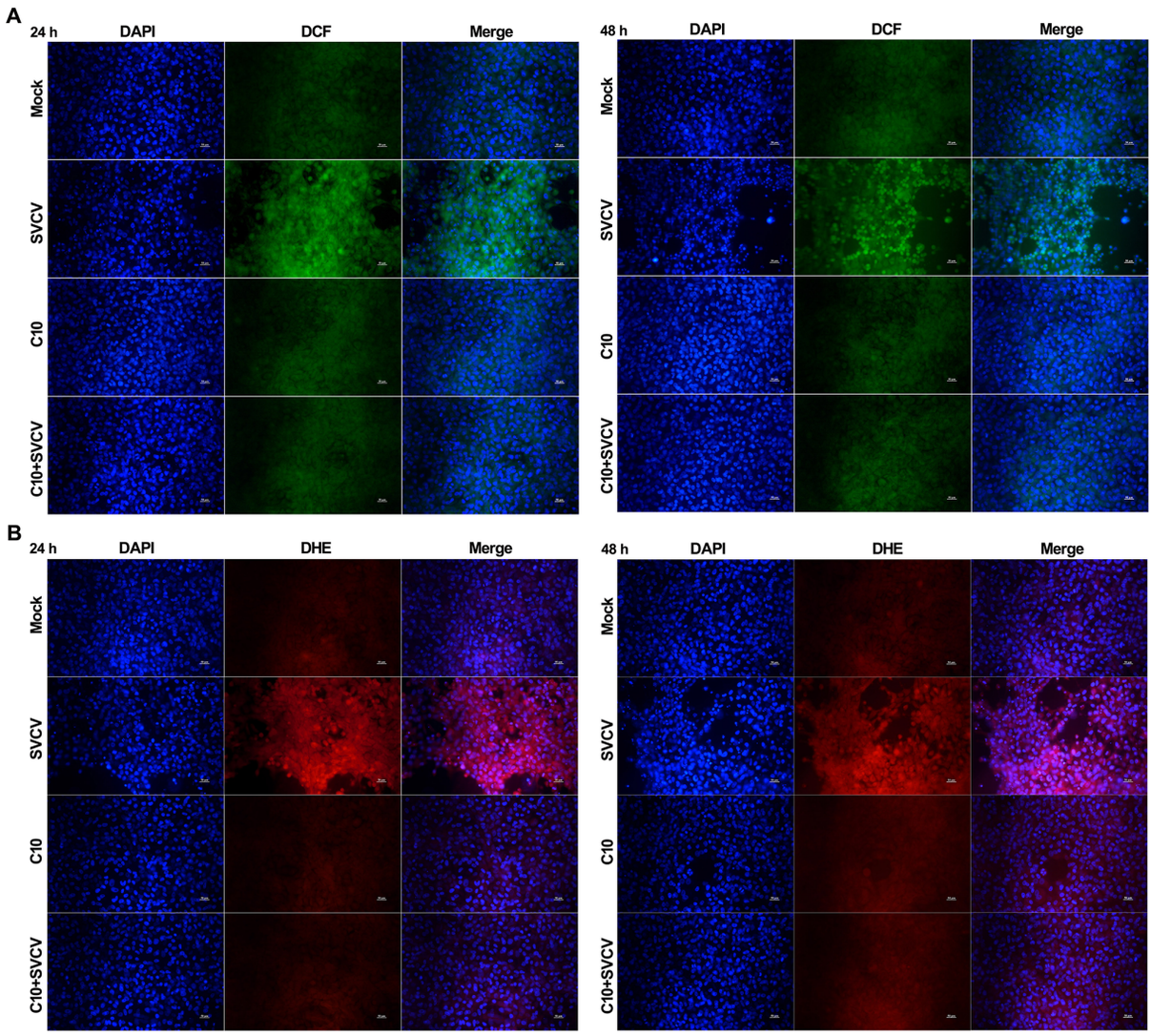

Figure 7 Anti-ROS effects of C10 in SVCV-infected cells

A: ROS levels in C10/SVCV-incubated EPC cells were examined with DCFH-DA. B: Superoxides in C10/SVCV-incubated EPC cells were examined with DHE. Final concentrations of 10 μmol/L DCFH-DA and 5 μmol/L DHE were added to cultures, respectively. Afterwards, cells were incubated for 30 min at 37 °C. Fluorescence was measured within 60 min using upright fluorescence microscopy.

observed in zebrafish at antiviral concentrations up to 50 mg/L C10, including no prolonged lethargy, decreased respiration rate, loss of equilibrium, circling, swimming slowly or at bottom of container, or death. In this study, zebrafish were infected with SVCV for 12 h prior to injection of 50 mg/L C10. Results indicated that C10 effectively reduced the mortality of SVCV-infected zebrafish by 70% (P<0.001) (Figure 10A). In parallel, corresponding protein N expression and viral titer were also decreased by C10 treatment at all time points (Figure 10B), suggesting that C10 inhibited SVCV replication in zebrafish and efficiently protected fish in the early stage of virus infection.

Antiviral responses *in vivo*

RT-qPCR was performed to detect antiviral responses of innate immune genes in zebrafish. In addition to MHC-II at 48 h, other gene expression levels were significantly up-regulated in C10-treated fish at 24 h and 48 h (Figure 11A, B). It should be noted that SVCV resulted in the up-regulation of innate immune genes solely at 24 h, reflecting that the antiviral responses of zebrafish were weakened to different extents at 48 h and 96 h (Figure 11C). Nevertheless, the differences in aoc2, MX, RIG-I, IFNγ, and ISG15 expression were still significant between the presence and absence of C10 in the treatment of SVCV-infected zebrafish.

DISCUSSION

Due to the complexity of the aquaculture environment and unique transition of pathogens through water, antiviral drugs,

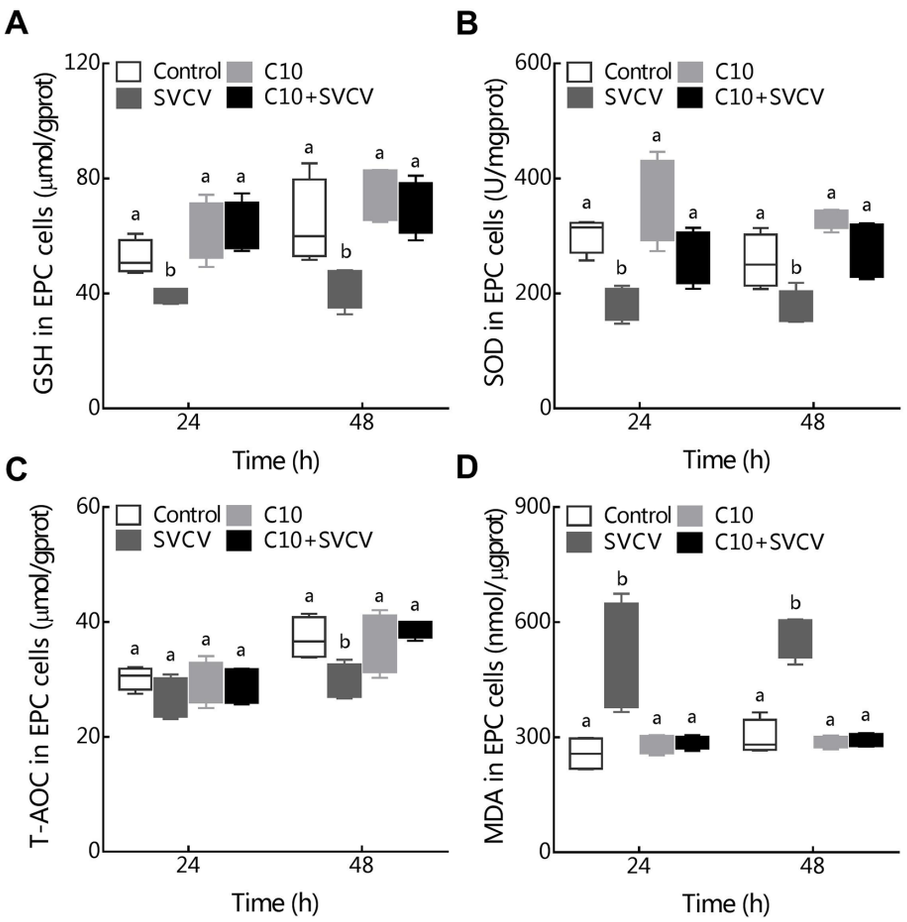

Figure 8 Antioxidative effects of C10 *in vitro*

Changes in GSH content (A), SOD activity (B), T-AOC (C), and MDA (D) contents in SVCV-infected cells after C10 treatment at 24 h and 48 h. Values are mean±*SD* from three replicates. *P*-values for each study were determined by Student's *t*-tests. **: $P<0.01$; *: $P<0.05$. Significance between control and exposure groups is indicated by letters.

especially broad-spectrum antivirals, are relatively limited (Liu et al., 2020). Although the situation may be challenging, new drugs are being developed to extend the limited arsenal of antivirals and to support medicinal improvement in the aquaculture environment. Structurally diverse coumarins display remarkable affinities to a variety of molecular targets for antiviral agents and slight modifications around the central motif can result in pronounced changes in its antiviral spectrum (Hassan et al., 2016). Previous study has shown that coumarin groups with linker lengths of three, four, and six carbon atoms have higher inhibitory effects on SVCV (Liu et al., 2017). These findings suggest that coumarins possess potential anti-SVCV properties. However, D4 (described in previous study of Liu et al. (2017)) only exhibits a maximum antiviral efficiency of <85% at a concentration of 10 mg/L, which is inconsistent with the structure-activity relationship analysis. In contrast, in the present study, C10, with the same structure as D4, was efficacious against SVCV *in vitro*, with a maximum antiviral response >97% at concentrations up to 12.5 mg/L and significantly inhibited SVCV replication in zebrafish at concentrations up to 50 mg/L. It is assumed that methylimidazole and benzimidazole with linker lengths of three, four, and six carbon atoms may play key roles in the anti-SVCV activity of coumarins. We considered that the variation may be related to the applied dose and purity of the synthetic compound. In addition to antiviral analysis through RT-qPCR on SVCV protein expression in EPC cells, other data, such as cell morphology, ultrastructure evaluation, apoptotic bodies, and ΔΨm levels, also confirmed high antiviral activity of C10 against SVCV in EPC cells. Although C10 did not reduce SVCV replication in the early stage of viral infection, it significantly reduced SVCV replication during viral biosynthesis, as observed in time-of-addition and time-of-removal analyses. Compared with other 7-hydroxy-imidazole coumarin medicines, such as 7-(3-benzimidazole propoxy) coumarin (B4) (Qiu et al., 2020), 7-(4-(4-methyl-imidazole))-coumarin (C2) (Liu et al., 2019a), 7-(4-benzimidazole-butoxy)-coumarin (BBC) (Liu et al., 2018; Shen et al., 2018), 4-phenyl-2-thioxo-1,2,3,4-tetrahydro-5H-chromeno[4,3-d] pyrimidin-5-one (S5) (Song et al., 2020) and 7-(6-(2-methyl-imidazole))-

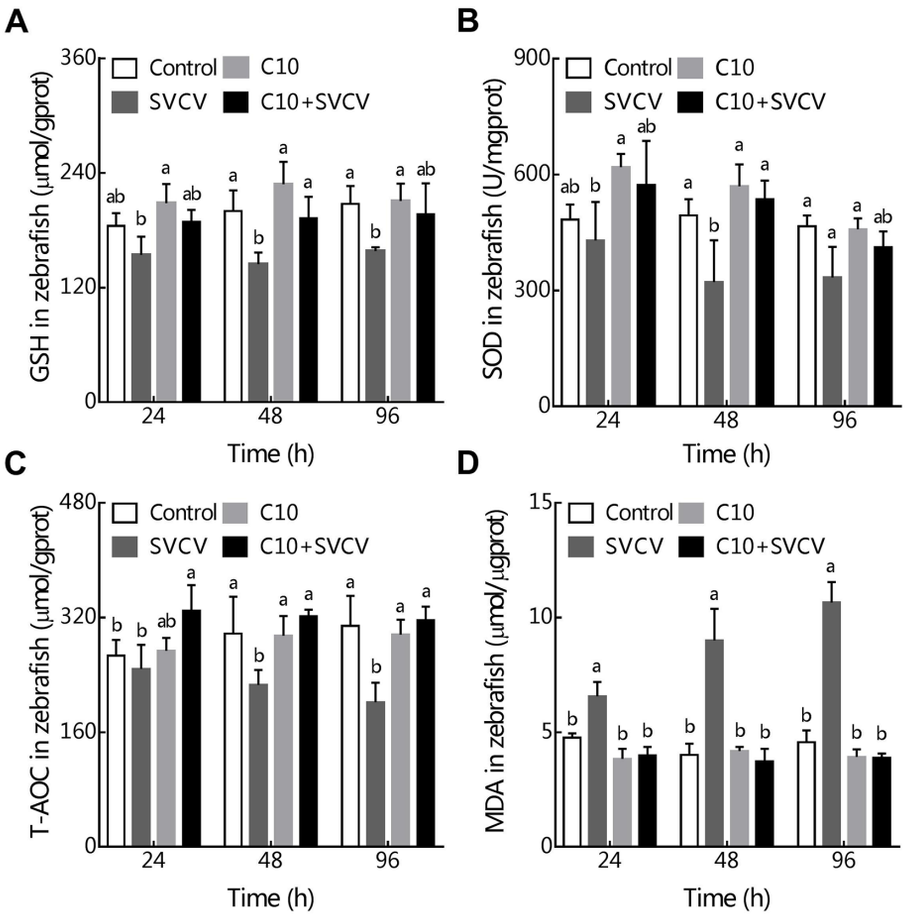

Figure 9 Antioxidative effects of C10 *in vivo*

Changes in GSH content (A), SOD activity (B), T-AOC (C), and MDA (D) contents in SVCV-infected cells after C10 treatment at 24 h and 48 h. Values are mean±*SD* from three replicates. *P*-values for each study were determined by Student's *t*-tests. **: $P<0.01$; *: $P<0.05$. Significance between control and exposure groups is indicated by letters.

coumarin (D5) (Liu et al., 2019b), C10 demonstrated lower acute toxicity in zebrafish, and could therefore be used as a viable agent for preventing and controlling SVCV infection.

In general, a virus triggers imbalance of intracellular redox cycling, resulting in ROS generation exceeding endogenous antioxidant defense in host cells. In contrast, the intracellular redox state can affect viral replication in host cells (Garaci et al., 1997; Michalek et al., 2008; Liu et al., 2018). It has been reported that prolonged stimulation with SVCV can disrupt the balance of intracellular redox cycling in fish (Yuan et al., 2012). Further study has speculated that some cytopathic effects may not be dependent on SVCV infection alone, but also induced by virus-mediated cell damage associated with oxidative stress (Yuan et al., 2014). Mechanistically, changes in several mitochondrial parameters after SVCV infection, including ultrastructural abnormalities, decreased ΔΨm levels, down-regulated MFN transcription, and varied activity of Complex I and Complex III, are suggestive of mitochondrial dysfunction (Zhao et al., 2018). Notably, in the current study, the number of mitochondria in SVCV-infected cells was reduced, revealing that SVCV replication may destroy mitochondria, leading to EPC cell apoptosis. Concomitantly, inactivation of mitochondria electron transport chain complex III to augment O^{2-} and H_2O_2 accumulation has also been observed in SVCV-infected EPC cells (Zhao et al., 2018). In response to ROS generation, antioxidant defense systems are activated against SVCV replication in the host (Shao et al., 2016). However, exponential enhancement of viral loads tends to break through defense easily and exceed the threshold in a time-dependent manner, resulting in serious damage in fish (Workenhe et al., 2010). Hydroxyl coumarins are regarded as antioxidant drugs in the formation and scavenging of ROS to induce the Nrf2-ARE signaling pathway against SVCV (Liu et al., 2017, 2018; Peng et al., 2013). In this sense, C10 treatment not only protected mitochondria, but also stimulated antioxidant capacity in zebrafish by maintaining antioxidant resistance, thereby simultaneously contributing to SVCV replication inhibition. Consequently, C10 protected zebrafish from SVCV-induced oxidative damage and enhanced survival.

Natural SVCV infection stimulates a robust early innate

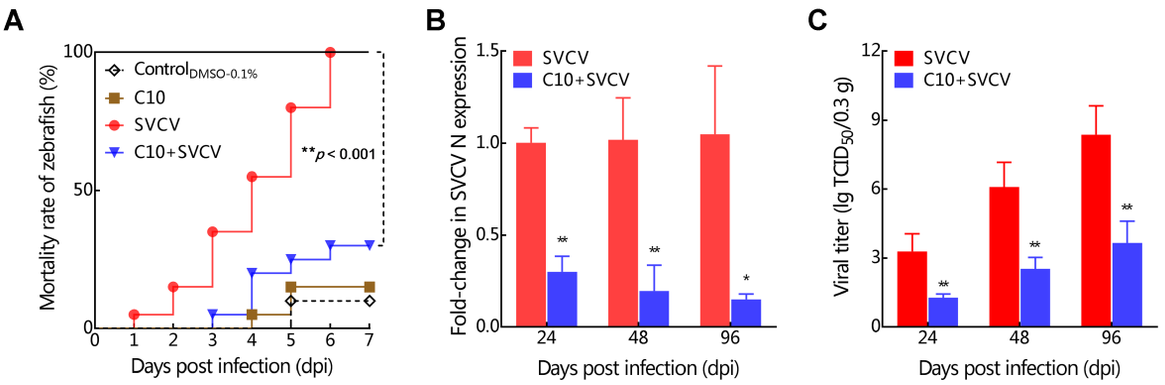

Figure 10 Antiviral effects of C10 in zebrafish

A: Survivorship curves of SVCV-infected fish under C10 treatments. Virus-infected fish were administered an intraperitoneal injection of C10 up to 50 mg/L and DMSO at a dose of 0.1% (v/v). B: Expression of SVCV N protein was examined by RT-qPCR in sampled fish. C: Viral loads were detected using median tissue culture infective dose (TCID50) analysis. Each value is mean±*SD* normalized to values for no treatment. *P*-values for each study were determined by Kaplan-Meier or Student's *t*-tests. **: *P*<0.01; *: *P*<0.05 (*n*=3 fish per treatment).

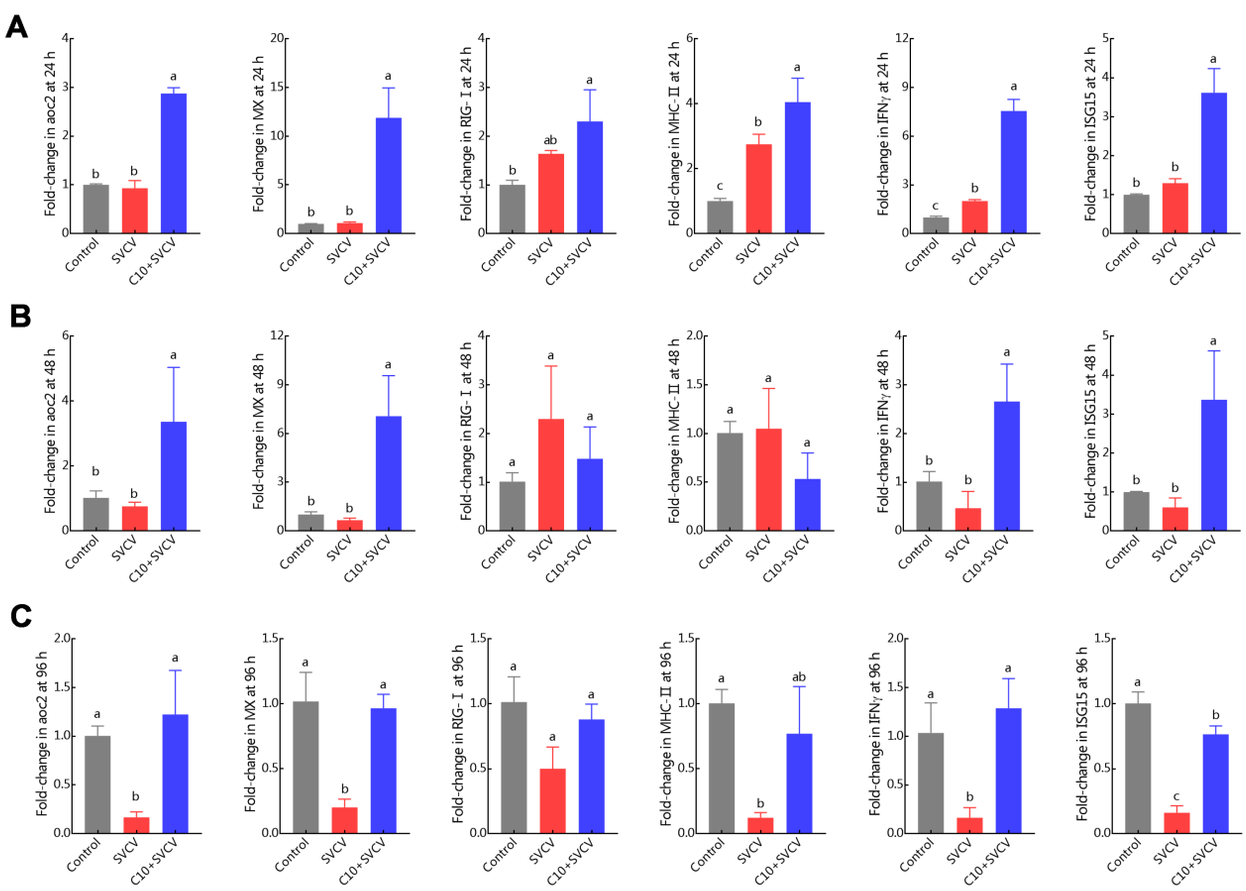

Figure 11 Antiviral responses of zebrafish in presence or absence of 12.5 mg/L C10 with SVCV infection

Relative RNA levels of IFN-related genes in sampled fish were determined by RT-qPCR at 24 h (A), 48 h (B), and 96 h (C). Each sample was run in triplicate normalized to 18S of zebrafish. Significance between control and exposure groups is indicated using alphabet (*n*=3 fish per treatment).

response, followed by a long-term specific immune response that is dependent on water temperature, virus dose, virus strain, and other host/virus factors (Balmer et al., 2017; Wang et al., 2017; Wei et al., 2016). As the first line of defense against pathogens, the response of the innate immune system to SVCV infection is mainly mediated by interferons (IFNs)

and IFN-induced proteins during the middle and late period of infection (Adamek et al., 2012; Forlenza et al., 2008). Virus-induced IFNs in fish form a group of genes, similar to those found in mammals, which play important antiviral roles in the innate immune system and trigger massive expression of IFN-stimulated genes (Aggad et al., 2009). Type I IFN in fish is produced and secreted by most types of infected cells, such as alarm proteins, the antiviral effects of which are exerted through the binding of interferon to specific cell-surface receptors to trigger signal transduction (Adamek et al., 2012). Subsequently, a wide array of interferon-stimulated genes (ISGs) are induced, which encode for antiviral proteins (Robertsen, 2006). In SVCV infection, RIG-I is also related to the strong activation of type I IFN, which binds viral RNA bearing a triphosphate at the 5' end and is associated with the mitochondrial antiviral signaling protein (MAVS), playing an important role in activating host antiviral responses in teleost fish (Chen et al., 2015). In addition, IFNγ in fish, a type II IFN, is more similar to IFNγ than to any of the other mammalian IFNs and displays powerful antiviral activities in zebrafish (López-Muñoz et al., 2009). Once virus-induced IFNs are synthesized and released, their receptors then bind to neighboring cells, with the resultant signaling transduction cascade stimulating antiviral proteins such as Mx (Cobbina et al., 2015). The results of the present study demonstrated that C10 activated IFN-related expression to negatively regulate SVCV replication in zebrafish during the early stage of infection. Interestingly, we found a gradual declining trend in the expression of six IFN-related genes, which appeared to be negatively correlated with SVCV replication in zebrafish. In fact, fish seemed to produce some resistance in the early stage of virus infection, whereas a degree of SVCV multiplication had a specific and immediate destructive effect conducive to its rapid proliferation. These results demonstrated that C10 not only maintained the antioxidant balance to delay virus-induced organism damage, but also indirectly cleared SVCV via IFN activation. Furthermore, a cycle was initiated, wherein low viral loads were consistently maintained in fish, benefiting the continuous activation of antiviral effects. According to previous studies (Shen et al., 2018; Liu et al., 2019), two coumarins, i.e., BBC and D5, up-regulate the expression of IFN-related genes in zebrafish without SVCV infection. We considered that C10 treatment alone up-regulated the expression of IFN-related genes because of its similar structure to BBC and D5. Therefore, these results suggested that C10 contributed to positive regulation of SVCV replication and proliferation in zebrafish.

In conclusion, C10 had a positive effect against SVCV infection *in vitro* and also showed good results *in vivo* by activating IFN response, maintaining redox state balance, and reducing zebrafish mortality. Collectively, our study highlights the potential of C10 as a therapeutic agent against SVCV infection in aquaculture.

COMPETING INTERESTS

The authors declare that they have no competing interests.

AUTHORS' CONTRIBUTIONS

J.C. drafted the experiments; L.L. and D.W.S. performed the experiments and wrote the paper. L.P.S. and T.X.Q. analyzed the data. All authors read and approved the final version of the manuscript.

REFERENCES

Adamek M, Rakus KŁ, Chyb J, Brogden G, Huebner A, Irnazarow I, Steinhagen D. 2012. Interferon type I responses to virus infections in carp cells: *in vitro* studies on Cyprinid herpesvirus 3 and *Rhabdovirus carpio* infections. *Fish & Shellfish Immunology*, **33**(3): 482−493.

Aggad D, Mazel M, Boudinot P, Mogensen KE, Hamming OJ, Hartmann R, Kotenko S, Herbomel P, Lutfalla G, Levraud JP. 2009. The two groups of zebrafish virus-induced interferons signal via distinct receptors with specific and shared chains. *The Journal of Immunology*, **183**(6): 3924−3931.

Ahne W, Bjorklund HV, Essbauer S, Fijan N, Kurath G, Winton JR. 2002. Spring viremia of carp (SVC). *Diseases of Aquatic Organisms*, **52**(3): 261−272.

Ashraf U, Lu YA, Lin L, Yuan JF, Wang M, Liu XQ. 2016. Spring viraemia of carp virus: recent advances. *Journal of General Virology*, **97**(5): 1037−1051.

Balmer BF, Powers RL, Zhang TH, Lee J, Vigant F, Lee B, Jung ME, Purcell MK, Snekvik K, Aguilar HC. 2017. Inhibition of an aquatic rhabdovirus demonstrates promise of a broad-spectrum antiviral for use in aquaculture. *Journal of Virology*, **91**(4): e02181-16.

Balmer BF, Getchell RG, Powers RL, Lee J, Zhang TH, Jung ME, Purcell MK, Snekvik K, Aguilar HC. 2018. Broad-spectrum antiviral JL122 blocks infection and inhibits transmission of aquatic rhabdoviruses. *Virology*, **525**: 143−149.

Bourinbaiar AS, Tan X, Nagorny R. 1993. Effect of the oral anticoagulant, warfarin, on HIV-1 replication and spread. *AIDS*, **7**(1): 129−130.

Bradford MM. 1976. A rapid and sensitive method for the quantitation of microgram quantities of protein utilizing the principle of protein-dye binding. *Analytical Biochemistry*, **72**(1-2): 248−254.

Chen HY, Liu WT, Wu SY, Chiou PP, Li YH, Chen YC, Lin GH, Lu MW, Wu JL. 2015. RIG-I specifically mediates group II type I IFN activation in nervous necrosis virus infected zebrafish cells. *Fish & Shellfish Immunology*, **43**(2): 427−435.

Chen ZY, Liu H, Li ZQ, Wang M, Zhang QY. 2006. Detection of viral pathogen from diseased common carp (*Cyprinus carpio*) by infectious tests. *Journal of Fishery Sciences of China*, **13**(4): 617−623. (in Chinese)

Cobbina SJ, Xu H, Zhao T, Mao GH, Zhou ZX, Wu XS, Liu HY, Zou YM, Wu XY, Yang LQ. 2015. A multivariate assessment of innate immune-related gene expressions due to exposure to low concentration individual and mixtures of four kinds of heavy metals on zebrafish (*Danio rerio*) embryos. *Fish & Shellfish Immunology*, **47**(2): 1032−1042.

Dikkeboom AL, Radi C, Toohey-Kurth K, Marcquenski S, Engel M, Goodwin AE, Way K, Stone DM, Longshaw C. 2004. First report of spring viremia of carp virus (SVCV) in wild common carp in North America. *Journal of*

Aquatic Animal Health, **16**(4): 169−178.
Encinas P, Garcia-Valtanen P, Chinchilla B, Gomez-Casado E, Estepa A, Coll J. 2013. Identification of multipath genes differentially expressed in pathway-targeted microarrays in zebrafish infected and surviving spring viremia carp virus (SVCV) suggest preventive drug candidates. *PloS One*, **8**: e73553.
Fijan N. 1984. Vaccination of fish in European pond culture: prospects and constraints. *Symposia Biologica Hungaria*, **23**: 233−241.
Forlenza M, de Carvalho Dias JD, Veselý T, Pokorová D, Savelkoul HFJ, Wiegertjes GF. 2008. Transcription of signal-3 cytokines, IL-12 and IFNαβ, coincides with the timing of CD8αβ up-regulation during viral infection of common carp (*Cyprinus carpio* L.). *Molecular Immunology*, **45**(6): 1531−1547.
Fujioka H, Yamasaki K, Furusawa K, Tamura K, Oguro K, Kurihara S, Seki S, Oshima SI, Imajoh M. 2015. Prevalence and characteristics of Cyprinid herpesvirus 3 (CyHV-3) infection in common carp (*Cyprinus carpio* L.) inhabiting three rivers in Kochi Prefecture, Japan. *Veterinary Microbiology*, **175**(2-4): 362−368.
Garaci E, Palamara AT, Ciriolo MR, D'Agostini C, Ab del-Latif MS, Aquaro S, Lafavia E, Rotilio G. 1997. Intracellular GSH content and HIV replication in human macrophages. *Journal of Leukocyte Biology*, **62**(1): 54−59.
Garver KA, Dwilow AG, Richard J, Booth TF, Beniac DR, Souter BW. 2007. First detection and confirmation of spring viraemia of carp virus in common carp, *Cyprinus carpio* L., from Hamilton Harbour, Lake Ontario, Canada. *Journal of Fish Diseases*, **30**(11): 665−671.
Hassan MZ, Osman H, Ali MA, Ahsan MJ. 2016. Therapeutic potential of coumarins as antiviral agents. *European Journal of Medicinal Chemistry*, **123**: 236−255.
Huang L, Kashiwada Y, Cosentino LM, Fan S, Chen CH, McPhail AT, Fujioka T, Mihashi K, Lee KH. 1994a. Anti-AIDS agents. 15. Synthesis and anti-HIV activity of dihydroseselins and related analogs. *Journal of Medicinal Chemistry*, **37**(23): 3947−3955.
Huang L, Kashiwada Y, Cosentino LM, Fan S, Lee KH. 1994b. 3',4'-Di-*o*-(-)-camphanoyl-(+)-*cis*khellactone and related compounds: A. *New class of potent anti-HIV agents. Bioorganic & Medicinal Chemistry Letters*, **4**(4): 593−598.
Koutná M, Veselý T, Psikal I, Hůlová J. 2003. Identification of spring viraemia of carp virus (SVCV) by combined RT-PCR and nested PCR. *Diseases of Aquatic Organisms*, **55**(3): 229−235.
Liu GL, Wang CJ, Wang HF, Zhu LL, Zhang H, Wang YS, Pei CY, Liu L. 2019a. Antiviral efficiency of a coumarin derivative on spring viremia of carp virus *in vivo*. *Virus Research*, **268**: 11−17.
Liu L, Hu Y, Lu JF, Wang GX. 2019b. An imidazole coumarin derivative enhances the antiviral response to spring viremia of carp virus infection in zebrafish. *Virus Research*, **263**: 112−118.
Liu L, Hu Y, Shen YF, Wang GX, Zhu B. 2017. Evaluation on antiviral activity of coumarin derivatives against spring viraemia of carp virus in epithelioma papulosum cyprini cells. *Antiviral Research*, **144**: 173−185.
Liu L, Qiu TX, Song DW, Shan LP, Chen J. 2020. Inhibition of a novel coumarin on an aquatic rhabdovirus by targeting the early stage of viral infection demonstrates potential application in aquaculture. *Antiviral Research*, **174**: 104672.
Liu L, Shen YF, Hu Y, Lu JF. 2018. Antiviral effect of 7-(4-benzimidazole-butoxy)-coumarin on rhabdoviral clearance via Nrf2 activation regulated by PKCα/β phosphorylation. *Fish & Shellfish Immunology*, **83**: 386−396.
Liu L, Zhu B, Wang GX. 2015. Azoxystrobin-induced excessive reactive oxygen species (ROS) production and inhibition of photosynthesis in the unicellular green algae *Chlorella vulgaris*. *Environmental Science and Pollution Research*, **22**(10): 7766−7775.
Livak KJ, Schmittgen TD. 2001. Analysis of relative gene expression data using real-time quantitative PCR and the $2^{-\Delta\Delta C}_{T}$ method. *Methods*, **25**(4): 402−408.
López-Muñoz A, Roca FJ, Meseguer J, Mulero V. 2009. New insights into the evolution of IFNs: zebrafish group II IFNs induce a rapid and transient expression of IFN-dependent genes and display powerful antiviral activities. *The Journal of Immunology*, **182**(6): 3440−3449.
Michalek RD, Pellom ST, Holbrook BC, Grayson JM. 2008. The requirement of reactive oxygen intermediates for lymphocytic choriomeningitis virus binding and growth. *Virology*, **379**(2): 205−212.
Miller O, Fuller FJ, Gebreyes WA, Lewbart GA, Shchelkunov IS, Shivappa RB, Joiner C, Woolford G, Stone DM, Dixon PF, Raley ME, Levine JF. 2007. Phylogenetic analysis of spring virema of carp virus reveals distinct subgroups with common origins for recent isolates in North America and the UK. *Diseases of Aquatic Organisms*, **76**(3): 193−204.
Neyts J, De Clercq E, Singha R, Chang YH, Das AR, Chakraborty SK, Hong SC, Tsay SC, Hsu MH, Hwu JR. 2009. Structure-activity relationship of new anti-hepatitis C virus agents: heterobicycle-coumarin conjugates. *Journal of Medicinal Chemistry*, **52**(5): 1486−1490.
Peng XM, Damu GLV, Zhou CH. 2013. Current developments of coumarin compounds in medicinal chemistry. *Current Pharmaceutical Design*, **19**(21): 3884−3930.
Penta S. 2015. Advances in Structure and Activity Relationship of Coumarin Derivatives. Amsterdam: Academic Press.
Petty BD, Riggs AC, Klinger R, Yanong RP, Francis-Floyd R. 2002. Spring viremia of carp. Fact Sheet VM-142. Gainesville, FL: University of Florida Cooperative Extension Service, University of Florida.
Pizzi M. 1950. Sampling variation of the fifty percent end-point, determined by the Reed-Muench (Behrens) method. *Human Biology*, **22**(3): 151−190.
Qiu TX, Song DW, Shan LP, Liu GL, Liu L. 2020. Potential prospect of a therapeutic agent against spring viraemia of carp virus in aquaculture. *Aquaculture*, **515**: 734558.
Robertsen B. 2006. The interferon system of teleost fish. *Fish & Shellfish Immunology*, **20**(2): 172−191.
Sancho R, Márquez N, Gómez-Gonzalo M, Calzado MA, Bettoni G, Coiras MT, Alcamí J, López-Cabrera M, Appendino G, Muñoz E. 2004. Imperatorin inhibits HIV-1 replication through an Sp1-dependent pathway. *The Journal of Biological Chemistry*, **279**(36): 37349−37359.
Shao JH, Huang J, Guo YN, Li LJ, Liu X1, Chen XX, Yuan JF. 2016. Up-regulation of nuclear factor E2-related factor 2 (Nrf2) represses the replication of SVCV. *Fish & Shellfish Immunology*, **58**: 474−482.
Shen YF, Hu Y, Zhang Z, Liu L, Chen C, Tu X, Wang GX, Zhu B. 2019. Saikosaponin D efficiently inhibits SVCV infection *in vitro* and *in vivo*. *Aquaculture*, **504**: 281−290.
Shen YF, Liu L, Feng CZ, Hu Y, Chen C, Wang GX, Zhu B. 2018. Synthesis and antiviral activity of a new coumarin derivative against spring viraemia of carp virus. *Fish & Shellfish Immunology*, **81**: 57−66.
Song DW, Liu L, Shan LP, Qiu TX, Chen J, Chen JP. 2020. Therapeutic potential of phenylpropanoid-based small molecules as anti-SVCV agents in

aquaculture. *Aquaculture*, **526**: 735349.

Stubbs MT, Bode W. 1993. A player of many parts: the spotlight falls on thrombin's structure. *Thrombosis Research*, **69**(1): 1−58.

Teng Y, Liu H, Lv JQ, Fan WH, Zhang QY, Qin QW. 2007. Characterization of complete genome sequence of the spring viremia of carp virus isolated from common carp (*Cyprinus carpio*) in China. *Archives of Virology*, **152**(8): 1457−1465.

Wang YD, Zhang H, Lu YA, Wang F, Liu LY, Liu JX, Liu XQ. 2017. Comparative transcriptome analysis of zebrafish (*Danio rerio*) brain and spleen infected with spring viremia of carp virus (SVCV). *Fish & Shellfish Immunology*, **69**: 35−45.

Wang ZG, Tang XB, Li YM, Leu C, Guo L, Zheng XD, Zhu DL. 2008. 20-Hydroxyeicosatetraenoic acid inhibits the apoptotic responses in pulmonary artery smooth muscle cells. *European Journal of Pharmacology*, **588**(1): 9−17.

Wei XX, Li XZ, Zheng XC, Jia P, Wang JJ, Yang XL, Yu L, Shi XJ, Tong GX, Liu H. 2016. Toll-like receptors and interferon associated immune factors responses to spring viraemia of carp virus infection in common carp (*Cyprinus carpio*). *Fish & Shellfish Immunology*, **55**: 568−576.

Workenhe ST, Rise ML, Kibenge MJT, Kibenge FSB. 2010. The fight between the teleost fish immune response and aquatic viruses. *Molecular Immunology*, **47**: 2525−2536.

Yuan JF, Su N, Wang M, Xie P, Shi ZL, Li LJ. 2012. Down-regulation of heme oxygenase-1 by SVCV infection. *Fish & Shellfish Immunology*, **32**(2): 301−306.

Yuan JF, Yang Y, Nie HH, Li LJ, Gu WG, Lin L, Zou M, Liu XQ, Wang M, Gu ZM. 2014. Transcriptome analysis of epithelioma papulosum cyprini cells after SVCV infection. *BMC Genomics*, **15**(1): 935.

Zhang YN, Li ZC, Ge XN, Guo X, Yang HC. 2011. Autophagy promotes the replication of encephalomyocarditis virus in host cells. *Autophagy*, **7**(6): 613−628.

Zhao LT, Qi L, Li C, Li LJ, Jin L, Yuan JF. 2018. SVCV impairs mitochondria complex Ⅲ resulting in accumulation of hydrogen peroxide. *Fish & Shellfish Immunology*, **75**: 58−65.

Zorova LD, Popkov VA, Plotnikov EY, Silachev DN, Pevzner IB, Jankauskas SS, Babenko VA, Zorov SD, Balakireva AV, Juhaszova M, Sollott SJ, Zorov DB. 2018. Mitochondrial membrane potential. *Analytical Biochemistry*, **552**: 50−59.